Article

Hypoxia-Induced Pulmonary Injury—Adrenergic Blockade Attenuates Nitrosative Stress and Inflammation but Not Pulmonary Edema

Isabel Riha , Aida Salameh , Annekathrin Hoschke , Coralie Raffort , Julia Koedel , Beate Rassler [*]

Article

Hypoxia-Induced Pulmonary Injury—Adrenergic Blockade Attenuates Nitrosative Stress and Inflammation but Not Pulmonary Edema

Isabel Riha [1,†], **Aida Salameh** [2,†], **Annekathrin Hoschke** [1], **Coralie Raffort** [2], **Julia Koedel** [3] **and Beate Rassler** [1,*]

[1] Carl-Ludwig-Institute of Physiology, University of Leipzig, Leipzig, Germany; isabel.riha@yahoo.de (I.R.); anne.hoschke@web.de (A.H.)

[2] Department of Pediatric Cardiology, Heart Centre, University of Leipzig, Leipzig, Germany; Aida.Salameh@medizin.uni-leipzig.de (A.S.); coralieraffort@orange.fr (C.R.)

[3] Institute of Pathology, University of Leipzig, Leipzig, Germany; julia.koedel@medizin.uni-leipzig.de

* Correspondence: Beate.Rassler@medizin.uni-leipzig.de; Tel.: +49 341 9715565

† These authors contributed equally to this work.

Abstract: Hypoxia can induce pulmonary edema (PE) and inflammation. Furthermore, hypoxia depresses left ventricular (LV) inotropy despite sympathetic activation. Here, we investigated the role of nitrosative stress and cardiovascular dysfunction in hypoxic lung injury. Additionally, we studied effects of adrenergic blockade (AB) on hypoxia-induced pulmonary injury. Eighty-six female rats were exposed for 72 h to normoxia or normobaric hypoxia and received infusions with NaCl, prazosin, propranolol or prazosin-propranolol combination. We evaluated hemodynamic function and performed histological and immunohistochemical analyses of the lung. Hypoxia significantly depressed LV but not right ventricular (RV) inotropic and lusitropic functions. AB significantly decreased LV function both in normoxia and hypoxia. AB effects on RV were weaker. Hypoxic rats showed signs of moderate PE and inflammation. This was accompanied by elevated levels of tumor necrosis factor (TNF) ⍺ and nitrotyrosine, a marker of nitrosative stress in the lungs. In hypoxia, all types of AB significantly reduced both TNF⍺ and nitrotyrosine to normoxic levels. However, AB did not attenuate PE. Results suggest that hypoxia-induced sympathetic activation contributes to inflammation and nitrosative stress in the lungs but not to PE. We suggest that AB in hypoxia aggravates hypoxia-induced inotropic LV dysfunction and backlog into pulmonary circulation, thus promoting PE.

Keywords: normobaric hypoxia; adrenergic blockade; pulmonary edema; pulmonary inflammation; tumor necrosis factor α; nitrotyrosine; left and right ventricular catheterization

1. Introduction

Acute exposure to hypoxia can induce pulmonary edema (PE) as can often be observed after rapid ascents to high altitude. High-altitude pulmonary edema (HAPE) is considered to be non-cardiogenic edema caused by elevated pulmonary capillary pressure resulting from hypoxic pulmonary vasoconstriction (HPV) [1,2]. HPV mainly occurs in pulmonary resistance arterioles but has also been observed in venules [3–5]. While pulmonary areas with high HPV have a reduced capillary perfusion, relative overperfusion and increased capillary pressure occur in lung areas with mild HPV. Pathogenesis of HAPE is related to an uneven distribution of HPV [6].   If venous resistance in these areas is elevated, water accumulation in the lung and fluid filtration into pulmonary interstitium may ensue [7]. Chest radiographs or computerized tomography scans in HAPE patients show a patchy distribution of edema, which is in accordance with the assumption of a regionally heterogenous pulmonary perfusion in hypoxia [1]. Moreover, subjects who are prone to develop HAPE, often show enhanced HPV accompanied by an

excessive rise in pulmonary artery systolic pressure (PASP), which may aggravate fluid extravasation [8,9]. In less severe cases, HAPE is confined to the pulmonary interstitium. However, excessive increase in capillary pressure may cause ultrastructural damage to the alveolo-capillary walls resulting in a high-permeability form of edema – a mechanism referred to as capillary stress failure [10,11]. The increase in pulmonary capillary pressure and hence, formation of PE can be promoted by cardiac dysfunction such as an imbalance in the pumping function of the left and right ventricles. Previous rat studies showed that hypoxia decreased systolic pressure and contractility of the left ventricle (LV), while the inotropic function of the right ventricle (RV) was not compromised [12]. This resulted in a mismatch between LV and RV that increased the backlog into pulmonary circulation and the severity of PE [13].

The precise mechanisms of HPV are not completely understood. Reduced bioavailability of nitric oxide (NO) is considered to provide an important component to vasoconstriction [14–16]. In addition to its vasodilator properties, NO is also a potent scavenger of oxidizing radicals generated by peroxynitrite [17]. Low NO levels have been suggested to result from continual consumption by interaction between NO and the superoxide anion resulting in increased peroxynitrite formation [18,19]. Peroxynitrite radicals can induce DNA damage and apoptosis and are indicated by elevated levels of nitrotyrosine, an important marker of nitrosative stress [20]. Numerous studies on animals and humans indicated a close relationship between generation of reactive oxygen and nitrogen species and hypoxia-induced pulmonary inflammation and edema [21–25].

Hypoxia-induced PE is typically accompanied by inflammatory reactions in the lung [26,27]. This was confirmed in previous studies on rats in normobaric hypoxia. PE emerged after 6 h of hypoxia and deteriorated with prolonged exposure to hypoxia over 24 h [12]. It was accompanied by inflammation as demonstrated by increased expression of pro-inflammatory cytokines such as interleukin (IL)-6 and tumor necrosis factor (TNF)α [13,28]. The inflammation, however, is considered to be rather a consequence than a cause of PE, but may maintain and aggravate edema formation [29].

In addition, hypoxia induces activation of the sympathetic nervous system [30–32]. Increased sympathetic activation, mainly mediated via α-adrenergic efferent pathways, is considered to play an important role in pulmonary vasoconstriction [33]. However, strong sympathetic activation may induce PE even in normoxic conditions. In human pathology, neurogenic PE or PE as a complication of pheochromocytoma are well-known examples of catecholamine-induced PE [34–37]. In rats infused with norepinephrine (NE) or other adrenergic agonists, we observed development of moderate interstitial edema after 6-8 h of infusion, which was accompanied by histological signs of inflammation in the lungs and increased concentrations of proinflammatory cytokines in serum and pleural fluid. The edema became more severe by 24 h and also affected the alveoli. While treatment with the α-adrenergic agonist phenylephrine aggravated both edema and inflammation, infusion of the β-agonist isoproterenol attenuated and decelerated the formation of edema [38]. Under prolonged infusion of adrenergic agonists, regression of edema and inflammation was observed after 72 h, but we found elevated mRNA expression of collagens type I and III as well as histological signs of beginning fibrosis and mild vascular hypertrophy in the lungs [39]. We therefore hypothesized that adrenergic blockade (AB) might attenuate hypoxia-induced pulmonary injury including both edema and inflammation and that these beneficial effects would be strongest with α-AB.

The present study was performed to investigate whether hypoxia-induced pulmonary edema and inflammation are still present after 72 h of hypoxia. Similarly, hemodynamic function was examined for hypoxia-induced disturbances in order to assess their role in formation of hypoxic PE. In addition, we compared the effects on pulmonary edema and inflammation of AB in normoxia and hypoxia. Finally, we investigated whether nitrosative stress as indicated by increased levels of nitrotyrosine (NT) can be demonstrated in the lungs after 72 h of normobaric hypoxia.

2. Materials and Methods

2.1. Animal model

All experiments were performed on 86 female Sprague–Dawley rats supplied by Charles River (Sulzfeld, Germany). The body weight was 236 ± 1.3 g at the beginning of the study corresponding to an age of about 10-12 weeks. All animal protocols were approved by the Federal State Agency (Landesdirektion Sachsen, protocol number TVV 46/18). The experiments were conducted in accordance with the Guide for the Care and Use of Laboratory Animals published by the National Institutes of Health and with the "European Convention for the Protection of Vertebrate Animals used for Experimental and other Scientific Purposes" (Council of Europe No 123, Strasbourg 1985).

2.2. Study protocol

Animals were subdivided into two cohorts to be exposed to normoxia (N) or normobaric hypoxia (H) for 72 hours. For exposure to hypoxia, the animals were placed into a hypoxic chamber sized 65 × 105 × 50 cm. The gas mixture in the chamber contained 10% oxygen in nitrogen. A special equipment prevented penetration of ambient air during manipulations on the animals to keep the oxygen concentration in the chamber stable at 10 ± 0.5%. Normoxic animals remained under room air condition. Additionally, all animals received an intravenous infusion over the total experimental time. The normoxic and hypoxic cohorts were subdivided into 4 groups each. From both cohorts, one group was infused with 0.9% sodium chloride (NaCl) solution (N-NaCl, n = 12; H-NaCl, n = 16). The remaining groups (one group each from the normoxic and hypoxic cohort) were infused with the α-adrenergic blocker prazosin (PZ, 0.1 mg kg^{-1} h^{-1}; N-PZ, n = 8; H-PZ, n = 12), the β-adrenergic blocker propranolol (PR, 0.16 mg kg^{-1} h^{-1}; N-PR, n = 8; H-PR, n = 12) or a combination of the two (PZ+PR, 0.1 + 0.16 mg kg^{-1} h^{-1}, respectively; N-PZ+PR, n = 8; H-PZ+PR, n = 10).

Infusions were administered with automatic pumps (Infors AG, Basel, Switzerland) at a rate of 0.1 ml h^{-1} via an infusion catheter (Vygon, Aachen, Germany). The infusion catheter was inserted into the left jugular vein. This operation was performed in 2% isofluran anesthesia. After catheter insertion, the animals woke up and moved freely with access to tap water and rat chow diet (Altromin C100, Altromin GmbH, Lage, Germany). Exposure to hypoxic environment started immediately after catheter insertion.

2.3. Hemodynamic measurements

About 30–40 min before the end of the exposure time, the animals were anesthetized with an intraperitoneal injection of thiopental (Trapanal® 80 mg kg^{-1}). They were tracheotomized, and a polyethylene cannula was placed in the trachea. The RV was catheterized with a Millar® (Millar Instruments, Houston, TX) ultraminiature catheter pressure transducer (for more details see our previous publication [40]). For catheterization of the LV, we used a pressure-volume catheter (Millar Instruments, Houston, TX). Data acquisition and analysis was performed with the Power Lab and Lab Chart Software from ADInstruments (sales department FMI Föhr Medical Instruments GmbH, Seeheim, Germany). Parallel conductance was corrected by injection of isotonic saline solution (0.1 ml, 0.9% NaCl). In both ventricles, we determined systolic peak pressures in the left and right ventricles (LVSP, RVSP), maximal velocities of increase (dP/dtmax) and decrease in pressure (dP/dtmin) as measures of ventricular contractility and relaxation, respectively, and heart rate (HR). In addition, end-diastolic pressure (LV edP) and stroke volume (SV) were measured in the LV. SV was calibrated by the thermodilution method (for more details see [41]). After withdrawal of the LV catheter tip into the aorta, diastolic aortic pressure (DAP) was measured to calculate mean aortic pressure (MAP). Cardiac index (CI, body mass-related cardiac output) was determined by thermodilution using a thermosensitive 1.5F microprobe and a Cardiomax II computer (Columbus Instruments, Columbus, OH). The total peripheral resistance (TPR) was calculated by dividing MAP by CI. Hypoxic animals remained in hypoxia until completion of hemodynamic measurements.

2.4. Sampling of materials

After completion of the hemodynamic measurements, the abdominal cavity was opened by midline incision. Animals were sacrificed by drawing blood from the abdominal aorta. Then, we opened the

thoracic wall and collected pleural fluid. After ligation of the right main bronchus, a bronchoalveolar lavage (BAL) of the left lung was performed two times consecutively with 3 ml 0.9% NaCl each. The fluid was instilled via the tracheal cannula into the left lung and withdrawn immediately. The recovery rate was about 90% on average. The recovered BAL fluid was frozen and stored at -80 °C for BAL cytology and other analyses. The left lung was discarded thereafter. From the intact right lung, tissue samples were fixated in formalin for histological analysis. A piece of the middle lobe was taken for determination of wet-to-dry weight (W/D) ratio.

2.5. Lung histology

The formalin-fixated tissue samples of the right lung were embedded in paraffin, sliced, and stained with hematoxylin–eosin. Histological assessments were done by two independent investigators (I.R. and J.K.), who were blinded towards the treatment group. In the lung, they evaluated PE and congestion. For a detailed quantification of PE, the complete histological section of a lung was assessed. First, PE severity (expressed as PE score) in each area of the section was gauged visually by evaluating the width of alveolar septa and the definition of alveolar spaces. PE scores ranged from 0 (absent), 1 (mild: alveolar septa slightly thickened, alveolar space well defined), 2 (moderate: thickness of alveolar septa about double the normal width, alveolar space narrowed but still defined), to 3 (severe: alveolar spaces hardly determinable and/or alveolar edema). The PE index (PEI) was calculated by cumulating the products of PE score and proportionate area of each part of the histological preparation. The congestion index (ConI) was determined in analogous way.

2.6. Immunohistochemistry

The expressions of TNFα, a potent pro-inflammatory cytokine, and NT in the lung were determined using immunohistochemistry. Specimens from the right lung, fixed with 4% formalin, were embedded in paraffin, and 2 μm slices were cut. After mounting on microscopic slides, the samples were dewaxed and rehydrated. For determination of TNFα, the specimens were cooked in 0.01M citrate buffer (pH=6) and then blocked with bovine serum albumin (BSA) to saturate unspecific bindings. Antigen retrieval was performed according to [42]. Specimens were treated with rabbit monoclonal anti-TNFα primary antibody (1:100, Sigma-Aldrich, Taufkirchen, Germany) over night at 4°C. Next, specimens were washed again in phosphate buffer and the appropriate goat anti-rabbit secondary antibody (1:200, Sigma-Aldrich, Taufkirchen, Germany) labelled with horseradish peroxidase (HRP) was applied for 2 hours. After a further washing step, peroxidase reaction was carried out using the red chromogen 3-amino-9-ethylcarbazole (AEC, Dako, Hamburg, Germany) according to the manufacturer´s instruction. Cell nuclei were counterstained with haemalum.

For detection of NT, the dewaxed and rehydrated specimens were cooked in 0.01M citrate buffer (pH=6). After blockade with BSA to saturate unspecific bindings, the specimens were treated with mouse monoclonal anti-nitrotyrosine primary antibody (1:100, Merck-Millipore, Darmstadt, Germany) over night at 4°C. Thereafter, the specimens were washed and the appropriate HRP-labelled secondary goat anti-mouse antibody (1:200, Sigma-Aldrich, Taufkirchen, Germany) was applied for 2 h at room temperature. Subsequently, the specimens were washed again, and visualization of positive cells was performed with AEC red chromogen (Dako, Hamburg Germany). Cell nuclei were counterstained with haemalum. The specimens were investigated microscopically using the Axioimager M1 microscope from Zeiss (Carl Zeiss, Jena, Germany). For determination of TNFα, which is mainly located in the bronchial and peribronchial regions, photographs were taken from these regions using the AxioCam MRc 5 camera and the AxioVision Rel. 4.6 software (Carl Zeiss, Jena, Germany) at 5 × magnification. At least 10 pictures per animal were evaluated by a blinded observer (I.R.). For measurements in the pictures, the program ImageJ [43] was used. As TNFα is located within the cytosol, we determined the TNFα-positive area (given in μm^2). The expression of TNFα is given as TNFα-positive area related to the total lung area of the specimen (in per cent). For NT determination, the procedure was similar, but photographs were taken at 20 x magnification. From each animal, at least 50 photographs were evaluated to measure the total area of the specimen and the percentage of NT-positive area.

2.7. Lung wet to dry weight ratio

Lung tissue samples were weighed immediately after preparation (wet weight, W) and after drying in an oven at 75 °C for 48 h (dry weight, D). The W/D ratio served as a surrogate parameter of water accumulation in the lung.

2.8. BAL cytology

BAL fluid was centrifuged for 20 min at 1500 rpm in a cytocentrifuge. The cytologic preparation was stained with hematoxylin-eosin and evaluated by a pathologist (J.K.) who was not aware of the treatment of the animal. The number of macrophages, neutrophils, lymphocytes, and eosinophils were given in per cent of the total cell number.

2.9. Statistical analysis

Statistical analyses were carried out with the software package SigmaPlot Version 14.0 (Systat Software GmbH, Erkrath, Germany) for Windows. All groups were statistically compared using analysis of variance (ANOVA) procedures. At first, we performed a Shapiro–Wilk test of normality. If data were normally distributed, we used a one-way ANOVA with a post hoc test according to Fisher's method of least significant differences (LSD). If the data were not normally distributed, a Kruskal–Wallis ANOVA on ranks with a post-hoc test according to Dunn's method was applied. Both post hoc tests are multiple comparison procedures comparing all possible pairwise mean differences. P values < 0.05 were considered significant.

3. Results

3.1. Hemodynamic results

All hemodynamic results are presented in Table 1. In general, cardiac function, particularly LV function, was compromised under hypoxic conditions. Hypoxia significantly depressed the inotropic and lusitropic functions of LV. In animals without AB, LVSP decreased from 123 ± 3 mm Hg in normoxia to 103 ± 4 mm Hg in hypoxia (p = 0.005). Significant reductions were also found for LV dP/dt max as a measure of contractility and for stroke volume. MAP was also lower in hypoxic than in normoxic control rats. HR significantly decreased from 426 ± 8 min^{-1} in the N-NaCl group to 390 ± 6 min^{-1} in the H-NaCl group (p = 0.028). Consequently, CI was also significantly reduced in the hypoxic control group (265 ± 10 ml min^{-1} kg^{-1} as compared to 337 ± 14 ml min^{-1} kg^{-1} in the N-NaCl group). LV dP/dt min as indicator of relaxation was mildly decreased while LV edP was slightly elevated. In contrast, RV function was not compromised by hypoxia; on the contrary, RVSP was even slightly improved.

AB decreased LV function significantly even in normoxia. This effect was strongest with β-AB (alone or in combination with the α-blocker PZ). The effects on RV were weaker and mostly not significant. In hypoxia, LVSP was not further reduced by AB, but LV dP/dt max and LV dP/dt min decreased even more than without AB, in particular with β-AB. Similarly, stroke volume, HR and CI decreased further with AB compared to the hypoxic control group. TPR tended to increase under hypoxic conditions, above all with β-AB. (Table 1).

Table 1. Hemodynamic results.

Cohort	Normoxic cohort:				Hypoxic cohort:			
Group	N-NaCl	N-PZ	N-PR	N-PZ+PR	H-NaCl	H-PZ	H-PR	H-PZ+PR
LVSP	**106.9 ± 3.7**				**99.4 ± 2.4**			
[mmHg]	123.3 ± 3.4	99.9 ± 5.5 °°	102.2 ± 11.9 °	92.5 ± 5.2 °°°	103.5 ± 3.8 **	96.8 ± 4.4	95.5 ± 6.3	101.3 ± 5.5
LV dP/dtmax	**8748 ± 494**				**7142 ± 364** **			
[mmHg/s]	10419 ± 622	9912 ± 933	6943 ± 1029°°	6804 ± 908°°	8365 ±569*	7798 ± 755	5838 ± 551°°	5893 ± 858°
LV dP/dtmin	**-9534 ± 541**				**-8437 ± 413**			
[mmHg/s]	-11896 ± 468	-9328 ± 1170°	-8433 ± 1307 °°	-7136 ± 927°°°	-10176 ± 614	-9178 ± 801	-6957 ± 689°°	-6439 ± 788 °°°
Stroke volume	**194.7 ± 6.9**				**165.5 ± 6.5** **			
[µl]	215.3 ± 7.2	211.7 ± 6.8	167.4 ± 18.8 °	172.4 ± 13.2 °	185.6 ± 11.6 *	152.9 ± 8.8 ° **	143.5 ± 18.5 °	164.8 ± 12.3
LV edP	**5.74 ± 0.34**				**6.97 ± 0.25** ***			
[mmHg]	5.93 ± 0.54	6.50 ± 1.13	5.04 ± 0.54	5.52 ± 0.67	6.38 ± 0.35	7.06 ± 0.48	7.10 ± 0.34	7.69 ± 0.86
RVSP	**27.9 ± 0.7**				**30.8 ± 0.9 ***			
[mmHg]	30.9 ± 0.9	26.8 ± 1.1	27.7 ± 1.6	24.7 ± 1.0 °	34.3 ± 1.5	29.6 ± 1.9	28.3 ± 0.8	29.1 ± 2.6
RV dP/dtmax	**2201 ± 138**				**2096 ± 119**			
[mmHg/s]	2307 ± 183	2466 ± 280	2542 ± 444	1511 ± 66	2458 ± 192	2350 ± 247	1638 ± 99	1646 ± 309 °
RV dP/dtmin	**-1777 ± 114**				**-1692 ± 81**			
[mmHg/s]	-2098 ± 174	-1815 ± 214	-1503 ± 129	-1503 ± 315	-1928 ± 137	-1824 ± 181	-1377 ± 80	-1469 ± 191
Heart rate	**426.0 ± 7.7**				**390.0 ± 6.2** ***			
[min^{-1}]	441.8 ± 8.1	458.1 ± 11.2	423.9 ± 9.3	374.5 ± 21.1°°°	410.4 ± 8.3*	407.4 ± 11.1	359.6 ± 11.9*** °°°	367.7 ± 13.9°°
Cardiac index	**337.4 ± 14.5**				**264.8 ± 9.6** ***			
[ml min^{-1} kg^{-1}]	387.4 ± 11.8	360.2 ± 38.6	302.3 ± 27.7 °°	276.5 ± 25.9 °°°	312.7 ± 15.6 **	258.7 ± 12.9 *** °	243.4 ± 18.0 °°	245.0 ± 14.7 °°
MAP [mmHg]	**96.4 ± 3.5**				**91.0 ± 2.4**			
	109.6 ± 3.5	91.0 ± 5.7	92.7 ± 11.6	84.7 ± 5.0	91.4 ± 3.6	91.2 ± 4.8	87.1 ± 5.9	95.2 ± 5.7
TPR [mmHg °	**0.30 ± 0.01**				**0.38 ± 0.03** *			
min ° kg ° s^{-1}]	0.29 ± 0.01	0.26 ± 0.02	0.33 ± 0.07	0.31 ± 0.03	0.30 ± 0.02	0.35 ± 0.03	0.42 ± 0.08	0.40 ± 0.04

Values are given as means ± SEM. LV, RV: left and right ventricle, respectively. SP: systolic peak pressure; dP/dt max: maximal velocity of pressure increase; dP/dt min: maximal velocity of pressure decrease; edP: end-diastolic pressure; MAP: mean aortic pressure; TPR: total peripheral resistance. Cohort values are given in bold; group values are given in standard types. Significance marks: significant differences between corresponding normoxic and hypoxic groups/cohorts: * $p < 0.05$; ** $p < 0.01$; *** $p < 0.001$; significant differences between blocker groups and the related (normoxic or hypoxic) control are marked with circles: ° $p < 0.05$; °° $p < 0.01$; °°° $p < 0.001$.

3.2. Lung histology and W/D ratio

After 72 h of normobaric hypoxia, histology of the lungs showed a mild to moderate PE associated with signs of inflammation. The edema was largely confined to the interstitium while alveoli were scarcely affected. Noteworthy, even lungs of normoxic animals were not free from edema, but the edema was significantly more severe in the hypoxic cohort (p = 0.023, Figure 1). The most pronounced difference between normoxic and hypoxic groups was observed in the control groups (N-NaCl vs. H-NaCl: p = 0.003). Application of adrenergic blockers aggravated the edema in normoxic animals, this was even significant with PZ (p = 0.017) and PZ+PR (p = 0.041). In contrast to what we had expected, AB did not attenuate PE under hypoxic conditions. We found a slight reduction of PE in the H-PZ group. By contrast, PE was even slightly aggravated with PZ+PR and was significantly more severe in the H-PZ+PR than in the H-PZ group (p = 0.026, Figure 1). The edema was associated with congestion of blood. Congestion was more severe in the hypoxic than in the normoxic cohort (p = 0.05) and was most pronounced in the H-PZ+PR group (Figure 2). The W/D ratio of the lungs corresponded with the histological findings. In very rare cases, the W/D ratio was greater than 6, which is indicating severe alveolar edema. However, W/D ratio was significantly lower in the normoxic than in the hypoxic cohort (Table 2). Correspondingly, the amount of pleural fluid was slightly higher in most of the normoxic than in hypoxic groups, in particular with AB, indicating that fluid drainage from the lungs was more efficient under normoxia compared to hypoxic conditions (Table 2). BAL cytology showed unremarkable results characterized by a vast majority of macrophages (about 90%); the rest was attributable to lymphocytes, neutrophil granulocytes and a very small portion of eosinophil and basophil granulocytes (data not shown). This distribution of cells corresponded to normal BAL cytology findings in humans [44].

Table 2. Lung wet-to-dry weight (W/D) ratio and pleural fluid volume.

Cohort	Normoxic cohort:				Hypoxic cohort:			
Group	N-NaCl	N-PZ	N-PR	N-PZ+PR	H-NaCl	H-PZ	H-PR	H-PZ+PR
W/D ratio [%]	**4.82 (4.73; 4.96)**				**5.03 (4.83; 5.42) ****			
	4.96 (4.80; 5.59)	4.77 (4.68; 4.82)	4.85 (4.66; 4.98)	4.79 (4.68; 4.92)	4.99 (4.82; 5.44)	5.01 (4.97; 5.16)	5.43 4.94; 5.74)	4.93 (4.73; 5.14)
Pleural fluid volume [mL]	**0.18 (0.10; 1.68)**				**0.20 (0.10; 1.23)**			
	0.10 (0.05; 0.16)	1.90 (0.13; 5.25)	0.35 (0.08; 1.68)	0.63 (0.16; 3.68)	0.13 (0.04; 0.55)	0.20 (0.08; 2.10)	0.20 (0.10; 0.80)	0.23 (0.10; 0.13)

Values are given as medians (25th/75th percentile). Cohort values are given in bold; group values are given in standard types. Significance marks: significant differences between corresponding normoxic and hypoxic cohorts: ** $p < 0.01$.
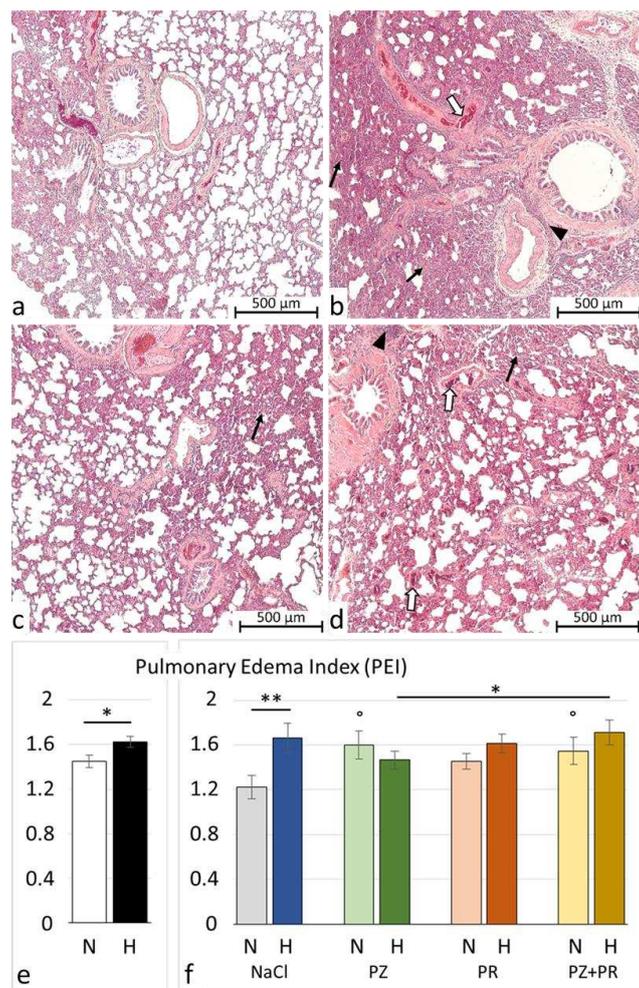
Figure 1. Pulmonary injury. (a-d) representative histological lung images (5 x magnification): (a) N-NaCl: largely unaffected lung with only mild edema and congestion; (b) H-NaCl: moderate to severe edema and inflammation, moderate congestion; (c) N-PZ+PR: mild to moderate edema and congestion, mild inflammation; (d) H-PZ+PR: moderate to severe edema and congestion, moderate inflammation. Pulmonary edema is marked by black arrows; inflammation is marked by white arrows; blood congestion is marked by arrowheads. (e, f) Pulmonary edema index of cohorts (e) and groups (f): N normoxia, H hypoxia, PZ prazosin, PR propranolol. Significance marks: — significant difference between marked columns, * P < 0.05; ** P < 0.01; ° significant difference to corresponding control (NaCl) group, P < 0.05.
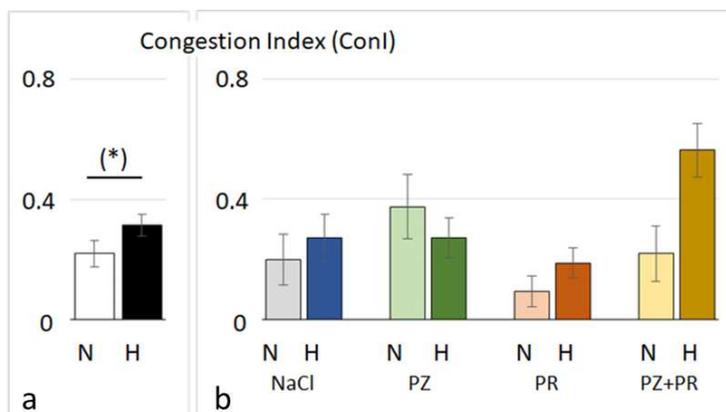
Figure 2. Lung congestion index of cohorts (a) and groups (b): N normoxia, H hypoxia, PZ prazosin, PR propranolol. Significance marks: (*) The difference between the normoxic and hypoxic cohorts is near to significance (P = 0.05).

3.3. Immunohistochemistry

Immunohistochemical analysis, however, revealed marked inflammation in the lungs as demonstrated by a significant increase in TNFα expression. The results showed a more than threefold percentage of TNFα-positive lung areas in the hypoxic cohort compared to the normoxic one. This difference was most pronounced in the control groups with a more than five-fold positive area in the H-NaCl group compared to N-NaCl animals (p < 0.001). AB had no effect in normoxic animals but attenuated TNFα expression in the hypoxic groups. This effect was particularly strong with single α-AB (H-PZ: p < 0.001 compared to H-NaCl; Figure 3).
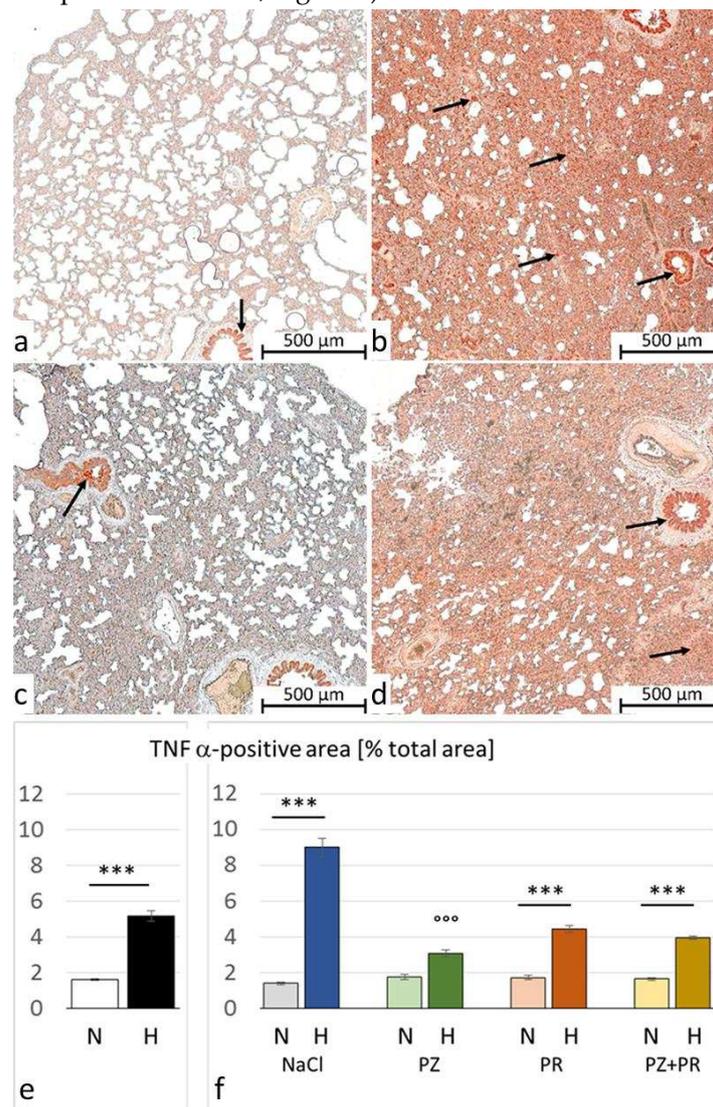

Figure 3. Tumor necrosis factor (TNF) α in the lung. (a-d) representative immunohistochemical images from N-NaCl (a), H-NaCl (b), N-PZ+PR (c) and H-PZ+PR (d), all slices 5 x magnification; red staining indicates TNFα-positive cells (examples are marked by arrows). (e, f) Abundance of TNFα of cohorts (e) and groups (f) expressed as percentage of positive area related to the total lung area: N normoxia, H hypoxia, PZ prazosin, PR propranolol. Significance marks: — significant difference between marked columns, *** P < 0.001; °°° significant difference to corresponding control (NaCl) group, P < 0.001.

Hypoxia induced nitrosative stress in the lungs as indicated by a significant increase in NT. In the hypoxic cohort, the percentage of NT-positive cells was more than three-fold the percentage in normoxic animals. In the H-NaCl group, NT-positive cells were more than four times the value in the N-NaCl group. Similar to inflammation, AB attenuated nitrosative stress under hypoxia. A significant reduction in the percentage of NT-positive cells as compared to the H-NaCl group was achieved with PZ (p = 0.002) and PZ+PR (p < 0.001). Of note, PZ+PR reduced NT even in normoxic conditions (p = 0.043; Figure 4).
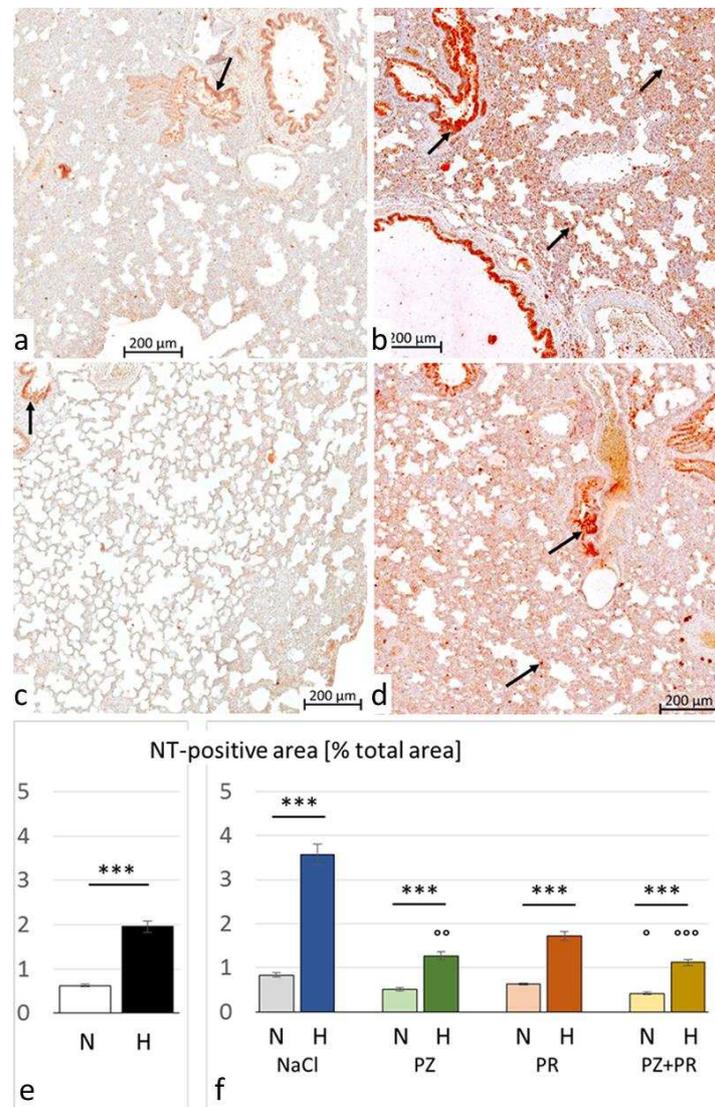

Figure 4. Nitrotyrosine (NT) in the lung. (a-d) representative immunohistochemical images from N-NaCl (a), H-NaCl (b), N-PZ+PR (c) and H-PZ+PR (d), all slices 20 x magnification; red staining indicates NT-positive cells (examples are marked by arrows). (e, f) Abundance of NT of cohorts (e) and groups (f) expressed as percentage of positive area related to the total lung area: N normoxia, H hypoxia, PZ prazosin, PR propranolol. Significance marks: — significant difference between marked columns, *** P < 0.001; ° significant difference to corresponding control (NaCl) group, P < 0.05, °° P < 0.01, P < 0.001.

4. Discussion

Our results showed that edema in the rat lung was still present after 72 h of exposure to normobaric hypoxia. The severity of PE was in a similar range or even slightly greater than observed in a previous study after 24 h of hypoxia [12]. This indicates that the processes involved in edema formation are still active and promote the progression of pulmonary injury. Uneven HPV associated

with elevated pulmonary capillary pressure are considered to be the main cause of hypoxic PE such as HAPE [1,6]. Of note, a specific effect of barometric pressure within the body is highly improbable, and the main causative factor for hypoxia-induced PE is not a reduction in barometric pressure but a reduction in inspiratory pO_2 [45] suggesting that pathogenesis of PE is comparable in normobaric and hypobaric hypoxia. Pulmonary vasoconstriction induces blood congestion in the pulmonary circulation as was also demonstrated in the hypoxic animals of the present study. An elevated end-diastolic pressure in the LV of hypoxic rats confirmed our assumption of a backlog from the LV into pulmonary circulation. Moreover, hypoxia affected the hemodynamics of the LV and RV in a differential manner, thus inducing a mismatch in the inotropic function of the LV and RV that aggravated pulmonary congestion. While LV systolic pressure and contractility were significantly reduced under hypoxic conditions, RV systolic pressure and contractility were maintained or even slightly improved.

Noteworthy, in contrast to our hypothesis, PE was not significantly attenuated by AB. And more, AB even aggravated PE under normoxic conditions. Hemodynamic results showed that AB, in particular with β-blockers, also compromised cardiac inotropic and lusitropic functions in normoxia. In general, the LV was more severely affected than the RV. As to be expected, β-AB (alone or in combination with the α-blocker PZ) exerted the most pronounced effects, particularly on LV contractility and relaxation. Isolated α-AB had weaker effects on LV function, but reduced TPR indicating a vasodilatory effect. Vasodilation in the pulmonary vasculature in combination with a reduced LV relaxation and slightly elevated LV edP suggest increased congestion in the pulmonary vascular bed [28]. These alterations of cardiovascular functions by adrenergic blockers and the resulting backlog into the lungs may explain the aggravation of PE.

In hypoxia, adrenergic blockers further deteriorated hypoxia-induced LV depression. Again, the depression was more pronounced with β-adrenergic blockers and predominantly concerned the LV. As a consequence, stroke volume decreased and LV edP increased compared to hypoxic animals with maintained adrenergic effects. The highest LV edP values were found in the H-PZ+PR group, and congestion index also reached its highest values in this group. These results confirm our suggestion that AB has reinforced the backlog into pulmonary circulation. This effect is even stronger in hypoxia than in normoxia and prevented the regression of edema.

Hypoxic PE is accompanied by inflammation in the lungs [26,27,46]. It is widely accepted that hypoxia-induced PE is not induced by inflammatory processes, but is maintained and aggravated by inflammation [29]. In rats, both acute and chronic hypobaric hypoxia induced pulmonary inflammation associated with a substantial increase in the serum levels of proinflammatory cytokines such as TNFα [47,48]. TNFα is a potent stimulator of inflammatory responses in many pulmonary diseases such as asthma, chronic obstructive pulmonary disease (COPD), acute lung injury/acute respiratory distress syndrome (ALI/ARDS) but also HAPE and high-altitude pulmonary hypertension (HAPH) [49,50]. In previous studies, we also found increased levels of TNFα in the lungs of rats exposed to normobaric hypoxia with an oxygen content of 10% over time intervals between 6 and 24 h [13,28]. The present results show that TNFα is still highly expressed after 72 h of hypoxia suggesting that inflammatory processes are still active and can maintain edema formation. Catecholamines are potent inflammatory activators of macrophages, upregulating production of cytokines such as TNFα via the NFκB pathway [51]. Proinflammatory effects of catecholamines or sympathetic activation are predominantly mediated by α-adrenergic stimulation while stimulation of β-adrenoceptors mainly induces anti-inflammatory effects [38,52]. However, β-adrenergic stimulation can also induce inflammation under certain conditions [53,54]. Previous studies on rats demonstrated that experimental infusion of NE and other adrenergic agonists induced pulmonary inflammation and upregulation of proinflammatory cytokines in serum and lung tissue [55,56]. Activation of the sympathetic nervous system under hypoxic conditions can make an important contribution to hypoxia-induced pulmonary inflammation. This was confirmed by our results demonstrating that sympathetic blockade, particularly α-AB with prazosin, significantly reduced TNFα levels in the lungs of hypoxic rats (see Figure 3).

Besides pulmonary edema and inflammation, hypoxia increases the generation of free radicals thus inducing oxidative/nitrosative stress. A study on rats revealed a significant increase in vascular

leakage, in proinflammatory cytokines such as IL-6 and TNFα, in the expression of NFkB and in reactive oxygen species in the lungs of rats exposed for up to 24 h to hypobaric hypoxia at 280 mmHg [22]. Moreover, animal studies demonstrated that hypoxia induced NO-synthase (NOS) isoforms in various organs, resulting in an increased production of peroxynitrite [20,57,58]. Peroxynitrite radicals induce nitrosylation of tyrosine residues, thus generating nitrotyrosines, which further can induce cell death.

Enhanced nitrosative stress, increased levels of TNFα and sympathetic stimulation are closely interrelated. TNFα is known to induce free radical generation and induction of oxidative/nitrosative stress [49,59] as could be demonstrated in various tissues including the lung [60–62]. From human pathology such as the Takotsubo syndrome, it is known that an excessive release of catecholamines can induce both inflammation and nitrosative stress [63]. Rat studies demonstrated that administration of adrenergic agonists increased both inflammation and nitrosative stress while AB attenuated it [64,65]. This is in accordance with our results demonstrating that reduction of TNFα levels in the lung by AB reduced in parallel also NT levels in pulmonary tissue. The results clearly show that hypoxic sympathetic activation makes a considerable contribution to hypoxia-induced lung injury.

5. Conclusions

The present results show that pulmonary edema and inflammation are still persistent after 72 h of normobaric hypoxia. This injury is associated with enhanced nitrosative stress as indicated by increased levels of nitrotyrosine in the lungs. AB, in particular α-AB, reduced the expression of TNFα in the lungs and attenuated pulmonary inflammation. This was accompanied by a reduction of nitrosative stress. However, these advantageous effects were not accompanied by attenuation of PE. This finding is in accordance with the pathogenetic concept of HAPE as this type of edema is formed independently of inflammation. The failure of AB to reduce pulmonary edema might be explained by the hemodynamic effects of AB aggravating the hypoxia-induced inotropic dysfunction of the LV and the backlog into the pulmonary circulation.

Abbreviation list:

AB   adrenergic blockade
ALI/ARDS   acute lung injury/acute respiratory distress syndrome
BAL   bronchoalveolar lavage
BSA   bovine serum albumin
CI   cardiac index
ConI   congestion index
COPD   chronic obstructive pulmonary disease
DAP   diastolic aortic pressure
dP/dtmax   maximal velocity of increase in pressure
dP/dtmin   maximal velocity of decrease in pressure
edP   end-diastolic pressure
H   normobaric hypoxia
HAPE   high-altitude pulmonary edema
HAPH   high-altitude pulmonary hypertension
HPV   hypoxic pulmonary vasoconstriction
HR   heart rate
IL   interleukin
LV   left ventricle/ventricular
MAP   mean aortic pressure
N   normoxia
NE   norepinephrine
NO   nitric oxide
NOS   nitric oxide synthase
NT   nitrotyrosine
PASP   pulmonary artery systolic pressure
PE   pulmonary edema

PEI	pulmonary edema index
PR	propranolol
PZ	prazosin
RV	right ventricle/ventricular
SP	systolic peak pressure
SV	stroke volume
TNF	tumor necrosis factor
TPR	total peripheral resistance
W/D ratio	wet-to-dry weight ratio

References

1. Bärtsch, P.; Mairbäurl, H.; Maggiorini, M.; Swenson, E.R. Physiological aspects of high-altitude pulmonary edema. *J. Appl. Physiol.* **2005**, 98,1101-1110. doi: 10.1152/japplphysiol.01167.2004.

2. Luks, A.M.; Swenson, E.R.; Bärtsch, P. Acute high-altitude sickness. *Eur. Respir. Rev.* **2017**, 26, 160096. doi: 10.1183/16000617.0096-2016.

3. Teboul, J.L.; Douguet, D.; Mercat, A.; Depret, J.; Richard, C.; Zelter, M. Effects of catecholamines on the pulmonary venous bed in sheep. *Crit. Care Med.* **1998**, 26, 1569-1575. doi: 10.1097/00003246-199809000-00027.

4. Maggiorini, M.; Mélot, C.; Pierre, S.; Pfeiffer, F.; Greve, I.; Sartori, C.; Lepori, M.; Hauser, M.; Scherrer, U.; Naeije, R. High-altitude pulmonary edema is initially caused by an increase in capillary pressure. *Circulation* **2001**, 103, 2078-2083. doi: 10.1161/01.cir.103.16.2078.

5. Gao, Y.; Raj, J.U. Role of veins in regulation of pulmonary circulation. *Am. J. Physiol. Lung Cell. Mol. Physiol.* **2005**, 288, L213-226. doi: 10.1152/ajplung.00103.2004.

6. Hopkins, S.R.; Levin, D.L. Heterogeneous pulmonary blood flow in response to hypoxia: a risk factor for high altitude pulmonary edema? *Respir. Physiol. Neurobiol.* **2006**, 151, 217-228. doi: 10.1016/j.resp.2005.10.007.

7. Younes, M.; Bshouty, Z.; Ali, J. Longitudinal distribution of pulmonary vascular resistance with very high pulmonary blood flow. *J. Appl. Physiol.* **1987**, 62, 344-358. doi: 10.1152/jappl.1987.62.1.344.

8. Hultgren, H.N.; Grover, R.F.; Hartley, L.H. Abnormal circulatory responses to high altitude in subjects with a previous history of high-altitude pulmonary edema. *Circulation* **1971**, 44, 759-770. doi: 10.1161/01.cir.44.5.759.

9. Grünig, E.; Mereles, D.; Hildebrandt, W.; Swenson, E.R.; Kübler, W.; Kuecherer, H.; Bärtsch, P. Stress Doppler echocardiography for identification of susceptibility to high altitude pulmonary edema. *J. Am. Coll. Cardiol.* **2000**, 35, 980-987. doi: 10.1016/s0735-1097(99)00633-6.

10. West, J.B.; Colice, G.L.; Lee, Y.J.; Namba, Y.; Kurdak, S.S.; Fu, Z.; Ou, L.C.; Mathieu-Costello, O. Pathogenesis of high-altitude pulmonary oedema: direct evidence of stress failure of pulmonary capillaries. *Eur. Respir. J.* **1995**, 8, 523-529.

11. West, J.B.; Mathieu-Costello, O. Structure, strength, failure, and remodeling of the pulmonary blood-gas barrier. *Annu. Rev. Physiol.* **1999**, 61, 543-572. doi: 10.1146/annurev.physiol.61.1.543.

12. Bölter, C.; Gabriel, P.; Appelt, P.; Salameh, A.; Schierle, K.; Rassler, B. Effects of Adrenergic Agonists and Antagonists on Cardiopulmonary Function During Normobaric Hypoxia in Rat. *Front. Physiol.* **2019**, 10, 860. doi: 10.3389/fphys.2019.00860.

13. Appelt, P.; Gabriel, P.; Bölter, C.; Fiedler, N.; Schierle, K.; Salameh, A.; Rassler, B. Left ventricular depression and pulmonary edema in rats after short-term normobaric hypoxia: effects of adrenergic blockade and reduced fluid load. *Pflugers Arch.* **2021**, 473, 1723-1735. doi: 10.1007/s00424-021-02618-y.

14. Berger, M.M.; Hesse, C.; Dehnert, C.; Siedler, H.; Kleinbongard, P.; Bardenheuer, H.J.; Kelm, M.; Bärtsch, P.; Haefeli, W.E. Hypoxia impairs systemic endothelial function in individuals prone to high-altitude pulmonary edema. *Am. J. Respir. Crit. Care Med.* **2005**, 172,763-767. doi: 10.1164/rccm.200504-654OC.

15. Bärtsch, P.; Gibbs, J.S. Effect of altitude on the heart and the lungs. *Circulation* **2007**, 116,2191-2202. doi: 10.1161/CIRCULATIONAHA.106.650796.

16. Scherrer, U.; Rexhaj, E.; Jayet, P.Y.; Allemann, Y.; Sartori, C. New insights in the pathogenesis of high-altitude pulmonary edema. *Prog. Cardiovasc. Dis.* **2010**, 52, 485-492. doi: 10.1016/j.pcad.2010.02.004.

17. Jourd'heuil, D.; Jourd'heuil, F.L.; Kutchukian, P.S.; Musah, R.A.; Wink, D.A.; Grisham, M.B. Reaction of superoxide and nitric oxide with peroxynitrite. Implications for peroxynitrite-mediated oxidation reactions in vivo. *J. Biol. Chem.* **2001**, 276, 28799-28805. doi: 10.1074/jbc.M102341200.

18. Hurst, J.K. Whence nitrotyrosine? *J. Clin. Invest.* **2002**, 109,1287-1289. doi: 10.1172/JCI15816.

19. Bowers, R.; Cool, C.; Murphy, R.C.; Tuder, R.M.; Hopken, M.W.; Flores, S.C.; Voelkel, N.F. Oxidative stress in severe pulmonary hypertension. *Am. J. Respir. Crit. Care Med.* **2004**, 169, 764-769. doi: 10.1164/rccm.200301-147OC.

20. Salameh, A.; Zöbisch, H.; Schröder, B.; Vigelahn, J.; Jahn, M.; Abraham, G.; Seeger, J.; Dähnert, I.; Dhein, S. Effects of Hypoxia and Acidosis on Cardiac Electrophysiology and Hemodynamics. Is NHE-Inhibition by Cariporide Still Advantageous? *Front. Physiol.* **2020**, 11, 224. doi: 10.3389/fphys.2020.00224.

21. Bakonyi, T.; Radak, Z. High altitude and free radicals. *J. Sports Sci. Med.* **2004**, 3, 64-69.

22. Sarada, S.; Himadri, P.; Mishra, C.; Geetali, P.; Ram, M.S.; Ilavazhagan, G. Role of oxidative stress and NFkB in hypoxia-induced pulmonary edema. *Exp. Biol. Med. (Maywood)* **2008**, 233, 1088-1098. doi: 10.3181/0712-RM-337.

23. Bailey, D.M.; Dehnert, C.; Luks, A.M.; Menold, E.; Castell, C.; Schendler, G.; Faoro, V.; Gutowski, M.; Evans, K.A.; Taudorf, S.; James, P.E.; McEneny, J.; Young, I.S.; Swenson, E.R.; Mairbäurl, H.; Bärtsch, P.; Berger, M.M. High-altitude pulmonary hypertension is associated with a free radical-mediated reduction in pulmonary nitric oxide bioavailability. *J. Physiol.* **2010**, 588, 4837-4847. doi: 10.1113/jphysiol.2010.194704.

24. Gao, H.; Tian, Y.; Wang, W.; Yao, D.; Zheng, T.; Meng, Q. Levels of interleukin-6; superoxide dismutase and malondialdehyde in the lung tissue of a rat model of hypoxia-induced acute pulmonary edema. *Exp. Ther. Med.* **2016**, 11, 993-997. doi: 10.3892/etm.2015.2962.

25. Paul, S.; Arya, A.; Gangwar, A.; Bhargava, K.; Ahmad, Y. Size restricted silymarin suspension evokes integrated adaptive response against acute hypoxia exposure in rat lung. *Free Radic. Biol. Med.* **2016**, 96, 139-151. doi: 10.1016/j.freeradbiomed.2016.04.020.

26. Kubo, K.; Hanaoka, M.; Hayano, T.; Miyahara, T.; Hachiya, T.; Hayasaka, M.; Koizumi, T.; Fujimoto, K.; Kobayashi, T.; Honda, T. Inflammatory cytokines in BAL fluid and pulmonary hemodynamics in high-altitude pulmonary edema. *Respir. Physiol.* **1998**, 111, 301-310. doi: 10.1016/s0034-5687(98)00006-1.

27. Madjdpour, C.; Jewell, U.R.; Kneller, S.; Ziegler, U.; Schwendener, R.; Booy, C.; Kläusli, L.; Pasch, T.; Schimmer, R.C.; Beck-Schimmer, B. Decreased alveolar oxygen induces lung inflammation. *Am. J. Physiol. Lung Cell. Mol. Physiol.* **2003**, 284, L360-367. doi: 10.1152/ajplung.00158.2002.

28. Kowalleck, U.; Ahmed, M.A.A.; Koedel, J.; Schierle, K.; Salameh, A.; Rassler, B. Relaxin does not prevent development of hypoxia-induced pulmonary edema in rats. *Pflugers Arch.* **2022**, 474, 1053-1067. doi: 10.1007/s00424-022-02720-9.

29. Swenson, E.R.; Maggiorini, M.; Mongovin, S.; Gibbs, J.S.; Greve, I.; Mairbäurl, H.; Bärtsch, P. Pathogenesis of high-altitude pulmonary edema: inflammation is not an etiologic factor. *J.A.M.A.* **2002**, 287, 2228-2235. doi: 10.1001/jama.287.17.2228.

30. Johnson, T.S.; Young, J.B.; Landsberg, L. Sympathoadrenal responses to acute and chronic hypoxia in the rat. *J. Clin. Invest.* **1983**, 71, 1263-1272. doi: 10.1172/jci110876.

31. Xie, A.; Skatrud, J.B.; Puleo, D.S.; Morgan, B.J. Exposure to hypoxia produces long-lasting sympathetic activation in humans. *J. Appl. Physiol.* **2001**, 91, 1555-1562. doi: 10.1152/jappl.2001.91.4.1555.

32. Hansen, J.; Sander, M. Sympathetic neural overactivity in healthy humans after prolonged exposure to hypobaric hypoxia. *J. Physiol.* **2003**, 546, 921-929. doi: 10.1113/jphysiol.2002.031765.

33. Duplain, H.; Vollenweider, L.; Delabays, A.; Nicod, P.; Bärtsch, P.; Scherrer, U. Augmented sympathetic activation during short-term hypoxia and high-altitude exposure in subjects susceptible to high-altitude pulmonary edema. *Circulation* **1999**, 99, 1713-1718. doi: 10.1161/01.cir.99.13.1713.

34. Šedý, J.; Kuneš, J.; Zicha, J. Pathogenetic Mechanisms of Neurogenic Pulmonary Edema. *J. Neurotrauma* **2015**, 32, 1135-1145. doi: 10.1089/neu.2014.3609.

35. Rachfalska, N.; Putowski, Z.; Krzych, Ł.J. Distant Organ Damage in Acute Brain Injury. *Brain Sci.* **2020**, 10, 1019. doi: 10.3390/brainsci10121019.

36. Dai, J.; Chen, S.J.; Yang, B.S.; Lü, S.M.; Zhu, M.; Xu, Y.F.; Chen, J.; Cai, H.W.; Mao, W. Recurrence of non-cardiogenic pulmonary edema and sustained hypotension shock in cystic pheochromocytoma. *J. Zhejiang Univ. Sci. B.* **2017**, 18, 449-452. doi: 10.1631/jzus.B1600411.

37. Y-Hassan, S.; Falhammar, H. Cardiovascular Manifestations and Complications of Pheochromocytomas and Paragangliomas. *J. Clin. Med.* **2020**, 9, 2435. doi: 10.3390/jcm9082435.

38. Rassler, B.; Reissig, C.; Briest, W.; Tannapfel, A.; Zimmer, H.G. Catecholamine-induced pulmonary edema and pleural effusion in rats--alpha- and beta-adrenergic effects. *Respir. Physiol. Neurobiol.* **2003**, 135, 25-37. doi: 10.1016/s1569-9048(03)00062-4.

39. Rassler, B.; Marx, G.; Schierle, K.; Zimmer, H.G. Catecholamines can induce pulmonary remodeling in rats. *Cell. Physiol. Biochem.* **2012**, 30, 1134-1147. doi: 10.1159/000343304.

40. Rassler, B.; Barth, W.; Zimmer, H.G. Transient pleural effusion in norepinephrine-stimulated rats. *Basic Res. Cardiol.* **2001**, 96, 471-477. doi: 10.1007/s003950170029.

41. Salameh, A.; Dhein, S.; Blanke, K.; Rastan, A.; Hiyasat, B.; Dietze, A.; Sobiraj, A.; Dähnert, I.; Janousek, J. Right or left ventricular pacing in young minipigs with chronic atrioventricular block: long-term in vivo cardiac performance; morphology; electrophysiology; and cellular biology. *Circulation* **2012**, 125, 2578-2587. doi: 10.1161/CIRCULATIONAHA.111.079087.

42. Dhein, S.; Grassl, M.; Gerdom, M.; Vollroth, M.; Bakhtiary, F.; von Salisch, S.; Krämer, K.; Sobiraj, A.; Kostelka, M.; Mohr, F.W.; Salameh, A. Organ-protective effects on the liver and kidney by minocycline in small piglets undergoing cardiopulmonary bypass. *Naunyn Schmiedebergs Arch. Pharmacol.* **2015**, 388, 663–676. doi: 10.1007/s00210-015-1115-4.

43. Abramoff, M.D.; Magalhaes, P.J.; Ram, S.J. Image processing with ImageJ. *Biophotonics Int.* **2004**, 11, 36–42.

44. de Blic, J.; Midulla, F.; Barbato, A.; Clement, A.; Dab, I.; Eber, E.; Green, C.; Grigg, J.; Kotecha, S.; Kurland, G.; Pohunek, P.; Ratjen, F.; Rossi, G. Bronchoalveolar lavage in children. ERS Task Force on bronchoalveolar lavage in children. European Respiratory Society. *Eur. Respir. J.* **2000**, 15, 217-231. doi: 10.1183/09031936.00.15121700.

45. Richalet, J.P. CrossTalk opposing view: Barometric pressure, independent of PO2, is not the forgotten parameter in altitude physiology and mountain medicine. *J. Physiol.* **2020**, 598, 897-899. doi: 10.1113/JP279160.

46. Hartmann, G.; Tschöp, M.; Fischer, R.; Bidlingmaier, C.; Riepl, R.; Tschöp, K.; Hautmann, H.; Endres, S.; Toepfer, M. High altitude increases circulating interleukin-6; interleukin-1 receptor antagonist and C-reactive protein. *Cytokine* **2000**, 12, 246-252. doi: 10.1006/cyto.1999.0533.

47. Arya, A.; Sethy, N.K.; Singh, S.K.; Das, M.; Bhargava, K. Cerium oxide nanoparticles protect rodent lungs from hypobaric hypoxia-induced oxidative stress and inflammation. *Int. J. Nanomedicine* **2013**, 8, 4507-45020. doi: 10.2147/IJN.S53032.

48. Rashid, M.; Fahim, M.; Kotwani, A. Efficacy of tadalafil in chronic hypobaric hypoxia-induced pulmonary hypertension: possible mechanisms. *Fundam. Clin. Pharmacol.* **2013**, 27, 271-278. doi: 10.1111/j.1472-8206.2011.01013.x.

49. Mukhopadhyay, S.; Hoidal, J.R.; Mukherjee, T.K. Role of TNFalpha in pulmonary pathophysiology. *Respir. Res.* **2006**, 7, 125. doi: 10.1186/1465-9921-7-125.

50. El Alam, S.; Pena, E.; Aguilera, D.; Siques, P.; Brito, J. Inflammation in Pulmonary Hypertension and Edema Induced by Hypobaric Hypoxia Exposure. *Int. J. Mol. Sci.* **2022**, 23, 12656. doi: 10.3390/ijms232012656.

51. Flierl, M.A.; Rittirsch, D.; Nadeau, B.A.; Sarma, J.V.; Day, D.E.; Lentsch, A.B.; Huber-Lang, M.S.; Ward, P.A. Upregulation of phagocyte-derived catecholamines augments the acute inflammatory response. *PLoS One* **2009**, 4, e4414. doi: 10.1371/journal.pone.0004414.

52. Bergmann, M.; Sautner, T. Immunomodulatory effects of vasoactive catecholamines. *Wien. Klin. Wochenschr.* **2002**, 114, 752-761.

53. Rassler, B. Role of α- and β-adrenergic mechanisms in the pathogenesis of pulmonary injuries characterized by edema; inflammation and fibrosis. *Cardiovasc. Hematol. Disord. Drug Targets* **2013**, 13, 197-207. doi: 10.2174/1871529x1303140129154602.

54. Pongratz, G.; Straub, R.H. The sympathetic nervous response in inflammation. *Arthritis Res. Ther.* **2014**, 16, 504. doi: 10.1186/s13075-014-0504-2.

55. Rassler, B.; Reissig, C.; Briest, W.; Tannapfel, A.; Zimmer, H.G. Pulmonary edema and pleural effusion in norepinephrine-stimulated rats--hemodynamic or inflammatory effect? *Mol. Cell. Biochem.* **2003**, 250, 55-63. doi: 10.1023/a:1024942132705.

56. Rassler, B.; Rohling, M.A.; Reissig, C.; Briest, W.; Tannapfel, A.; Zimmer, H.G. Involvement of cytokines and inflammation in catecholamine-induced pulmonary injury in rats. *Vasc. Dis. Prev.* **2005**, 2, 1-9.

57. van den Tweel, E.R.; Nijboer, C.; Kavelaars, A.; Heijnen, C.J.; Groenendaal, F.; van Bel, F. Expression of nitric oxide synthase isoforms and nitrotyrosine formation after hypoxia-ischemia in the neonatal rat brain. *J. Neuroimmunol.* **2005**, 167, 64-71. doi: 10.1016/j.jneuroim.2005.06.031.

58.   Evans, L.C.; Liu, H.; Pinkas, G.A.; Thompson, L.P. Chronic hypoxia increases peroxynitrite, MMP9 expression, and collagen accumulation in fetal guinea pig hearts. *Pediatr. Res.* **2012**, 71, 25-31. doi: 10.1038/pr.2011.10.

59.   Wang, Y.; Wang, X.; Lau, W.B.; Yuan, Y.; Booth, D.; Li, J.J.; Scalia, R.; Preston, K.; Gao, E.; Koch, W.; Ma, X.L. Adiponectin inhibits tumor necrosis factor-α-induced vascular inflammatory response via caveolin-mediated ceramidase recruitment and activation. *Circ. Res.* **2014**, 114, 792-805. doi: 10.1161/CIRCRESAHA.114.302439.

60.   Ferro, T.J.; Hocking, D.C.; Johnson, A. Tumor necrosis factor-alpha alters pulmonary vasoreactivity via neutrophil-derived oxidants. *Am. J. Physiol.* **1993**, 265, L462-471. doi: 10.1152/ajplung.1993.265.5.L462.

61.   Wang, Q.; Doerschuk, C.M. Neutrophil-induced changes in the biomechanical properties of endothelial cells: roles of ICAM-1 and reactive oxygen species. *J. Immunol.* **2000**, 164, 6487-6494. doi: 10.4049/jimmunol.164.12.6487.

62.   Corda, S.; Laplace, C.; Vicaut, E.; Duranteau, J. Rapid reactive oxygen species production by mitochondria in endothelial cells exposed to tumor necrosis factor-alpha is mediated by ceramide. *Am. J. Respir. Cell. Mol. Biol.* **2001**, 24, 762-768. doi: 10.1165/ajrcmb.24.6.4228.

63.   Lyon, A.R.; Citro, R.; Schneider, B.; Morel, O.; Ghadri, J.R.; Templin, C.; Omerovic, E. Pathophysiology of Takotsubo Syndrome: JACC State-of-the-Art Review. *J. Am. Coll. Cardiol.* **2021**, 77, 902-921. doi: 10.1016/j.jacc.2020.10.060.

64.   Surikow, S.Y.; Nguyen, T.H.; Stafford, I.; Chapman, M.; Chacko, S.; Singh, K.; Licari, G.; Raman, B.; Kelly, D.J.; Zhang, Y.; Waddingham, M.T.; Ngo, D.T.; Bate, A.P.; Chua, S.J.; Frenneaux, M.P.; Horowitz, J.D. Nitrosative Stress as a Modulator of Inflammatory Change in a Model of Takotsubo Syndrome. *J.A.C.C. Basic Transl. Sci.* **2018**, 3, 213-226. doi: 10.1016/j.jacbts.2017.10.002.

65.   Schäper, J.; Wagner, A.; Enigk, F.; Brell, B.; Mousa, S.A.; Habazettl, H.; Schäfer, M. Regional sympathetic blockade attenuates activation of intestinal macrophages and reduces gut barrier failure. *Anesthesiology* **2013**, 118,134-142. doi: 10.1097/ALN.0b013e3182784c93.